Exp Brain Res (1991) 86:209–215

Experimental Brain Research

Listing's law for eye, head and arm movements and their synergistic control

D. Straumann[1], Th. Haslwanter[1], M.-C. Hepp-Reymond[2], and K. Hepp[3]

[1] Neurology Department, University Hospital, CH-8091 Zürich, Switzerland
[2] Brain Research Institute, University, CH-8029 Zürich, Switzerland
[3] Physics Department, ETH, CH-8093 Zürich, Switzerland

Received January 3, 1991 / Accepted April 8, 1991

Summary. We have recorded eye, head, and upper arm rotations in five healthy human subjects using the three-dimensional search coil technique. Our measurements show that the coordination of eye and head movements during gaze shifts within ± 25 deg relative to the forward direction is organized by restricting the rotatory trajectories of the two systems to almost parallel planes. These so-called "Listing planes" for eye-in-space and head-in-space rotations are workspace-oriented, not body-fixed. Eye and head trajectories in their respective planes are closely related in direction and amplitude. For pointing or grasping, the rotatory trajectories of the arm are also restricted to a workspace-oriented Listing plane. During visually guided movements, arm follows gaze, and the nine-dimensional rotatory configuration space for eye-head-arm-synergies (three degrees of freedom for each system) is reduced to a two-dimensional plane in the space of quaternion vectors.

Key words: Eye-Head-Arm-Coordination – Gaze – Rotatory synergy – Reaching – Human

Introduction

Human motor control in the multi-dimensional configuration space of limb movements appears to be so remarkably flexible and easy. Yet the underlying neural operations are only vaguely understood, even for the well-studied eye-head-arm-synergies (Jeannerod 1988). One of the guiding principles of motor behavior is the existence of stereotyped motor programs with only a few control parameters, by which we can "master the redundant degrees of freedom of the moving organ" (Bernstein 1967, p. 127).

An important example of reducing the dimensionality of the motor control space is Listing's law for eye movements (Helmholtz 1866): Let every eye position be described by one rotation of the eye ball from a reference position in a head-fixed coordinate system. Then each instantaneous eye position during fixations has its rotation axis in a head-fixed plane, called Listing plane, if the head is upright and stationary. Since Listing's law also applies to saccadic eye movements (Ferman et al. 1987; Tweed and Vilis 1990), it provides a unique correspondence between eye trajectories and the two-dimensional retinal coordinates of vision, and allows an efficient neural coding of saccades by two-dimensional motor maps in the superior colliculus and frontal eye fields (Hepp 1990).

Recently, it has been reported that also head (Tweed and Vilis 1988) and arm (Hepp and Hepp-Reymond 1989) show properties which can be described by Listing's law. With the conjecture that Listing's law might be fundamental for the neural control of certain classes of motor programs involving rotations, we have investigated the synergistic movements of eye, head, and arm in three dimensions.

Offprint requests to: D. Straumann (address see above)

Methods

In five healthy right-handed human subjects we have measured rotations of eye, head, and arm using three-dimensional magnetic search coils. Informed consent was obtained from all subjects (three experimenters, two naive subjects) after the procedures were fully explained. The magnetic search coil technique was originally developed for the recording of eye movements (Robinson 1963). We used two coupled Eye Position Meters Type 3000 (Skalar Instruments, Delft, The Netherlands) to measure the rotations of two dual search coils (manufactured by Skalar Instruments according to specifications by Dr. H. Collewijn). The side length of the magnetic coil frame was 70 cm; search coils could be displaced up to 10 cm from the center of the magnetic fields with a resulting position error of less than 10 percent. By the experimental setup (see below) we ensured that the coils remained inside this 10 cm range from the center, even during combined gaze-arm measurements. Raw voltage signals were sampled with a rate of 833 Hz and analyzed off-line.

Search coils were placed around the cornea, on the forehead, and rigidly fixed to the upper arm. Any two of the three rotatory systems could be measured simultaneously. Subjects were seated upright in the space-fixed magnetic field configuration and instruct-

ed to keep their backs to the chair. By frequent visual inspection and careful choice of the workspace, we made sure that the shoulders and the elbow angles were approximately fixed during experiments.

"Arm rotation" was defined as the rotation of the humerus. This rotation is equivalent to the orientation of the triangle spanned by wrist, elbow, and shoulder. Coils placed on the forearm would yield a combination of upper arm rotation and pronation/supination. However, the latter movement is mainly involved in the torsional hand orientation. We mounted the coil on the proximal end of a plastic bar, which was fixed to the dorsal upper arm directly above the elbow joint extending towards the shoulder. With this technique we made sure that during arm movements the coil remained inside the homogeneous part of the magnetic field. The chosen arm area for fixating the bar showed the least skin displacement relative to the humeral bone during movements.

The calibration of the raw search coil signals included three steps: (1) In an "in-vitro calibration" before each experiment, we mounted the dual search coil annulus on a gimbal system and determined sensitivity and orientation of both coils by measuring the induced voltages at well-defined gimbal positions. (2) During each experiment "in-vivo calibrations" were repeated every 5 min. This practice made it easy to detect possible slips of the eye coil and displacements of head or upper arm coils out of the homogenous part of the magnetic field; hence, every calibration trial gave new reference values for the experimental runs performed thereafter. For the calibration of head or arm, two parallel low-weight lasers were fixed near the coil; the subjects were asked to point with one laser-beam to vertically arranged dots on the screen. The second laser was used to keep the amount of limb-torsion constant during the task. From the induced search coil voltages we were able to compute the orientation of the coils in the reference position and their electronic offsets, using also the values obtained from the in-vitro calibration. For the eye calibration the procedure was similar; here, we relied on Listing's law and assumed that torsional changes during vertical fixations were small. The precise algorithm is described elsewhere (Hess et al. in prep.) (3) Off-line, we related each experimental trial to the reference values of the last in-vivo calibration. For every sample point, we calculated the orientations of both coil vectors, taking into account the voltage offsets and the lengths of the two coil vectors given by the in-vivo calibration. Then we computed the rotation which was needed to turn the pair of coil vectors from the reference position into the instantaneous position.

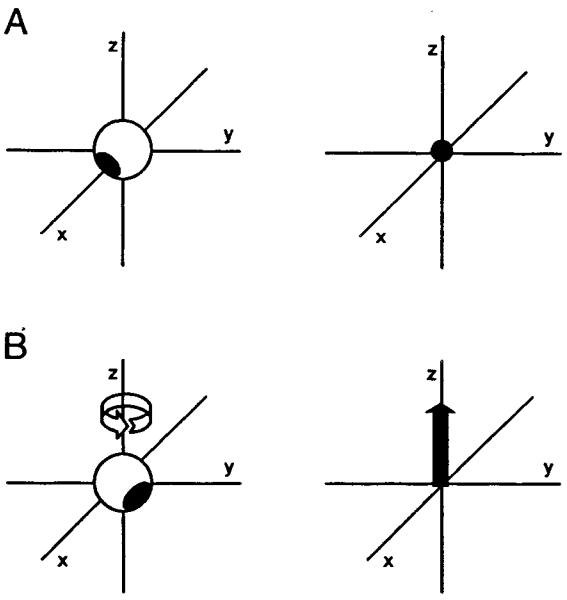

Fig. 1. Parametrization of eye position by a rotation from the reference position. The left column illustrates the eye in its reference position and in a horizontal position 20 deg to the left. The right column shows the quaternion vectors for these two positions. The length of a quaternion vector is given by the amount of rotation from the reference position; the vector points along the rotation axis. For the reference position the quaternion vector is (0,0,0). Note that the coordinate system does not rotate with the eye; therefore, the torsional component of a quaternion vector taken alone is not a rotation about the line of sight but a rotation about the x-axis. According to the right hand rule, the x-axis of the coordinate system points forward, the y-axis leftward, and the z-axis upward; positive values of quaternion vector components are assigned with leftward, downward, or clockwise rotations (as seen by the subject)

A typical experimental run lasted 50 s, during which subjects repeatedly gazed, pointed or grasped within a workspace of 50 deg angular diameter. The orientation of the body relative to the workspace could be changed by rotating the chair inside the magnetic field about the vertical axis. Eye, head, and arm movements towards spatially distributed targets were either self-paced or triggered by dots which were randomly projected on a tangent screen. In most experiments, arm movements were performed under visual control, with the head unrestrained. Experiments included "saccadic"[1] and pursuit tasks.

Every task was repeated 2–4 times by each subject. All analyzed data of a task were pooled for the five subjects. For statistical statements the following parameters are given: mean ± standard deviation, range, number of pooled runs (N). In calculating the standard deviation, we divided by N.

Eye, head, and arm rotations were characterized by quaternion vectors q = sin(rho/2)e, where the unit vector e describes the axis of rotation from the reference position and rho the angle of rotation (Westheimer 1957; Tweed and Vilis 1987). A quaternion vector consists of the three spatial components of a unit quaternion. x denotes the torsional, y the vertical, and z the horizontal component of a rotation. Figure 1 shows two examples of eye position with the corresponding quaternion vectors. In the following, the term "plane" or "Listing plane" will always refer to the best-fit plane through the data of one experimental run in the space of quaternion vectors.

Results

In a first series of experiments we studied eye-head-coordination during head-unrestrained gaze shifts to displayed targets. Figure 2 shows the quaternion vectors of eye-in-space (= gaze) (2A) and head-in-space (2B) rotations during a typical run of gaze saccades. The reference coordinate system is given by the space-fixed magnetic coil frame. The subject looks at laser dots which randomly appear at different locations on the screen. From the rotations of eye and head relative to space we computed eye rotations relative to the head (2C) using the equation:

$$e = g\sqrt{1-\|h\|^2} - h\sqrt{1-\|g\|^2} + g \times h$$

where e, g and h are the quaternion vectors for eye, gaze and head, and " × " denotes the vector product[2]. As one can see in the frontal and side display of the quaternion vectors, the rotatory trajectories for gaze, head, and eye are approximately confined to Listing planes, i.e. torsional rotations (x-axis) are very small compared to horizon-

[1] i.e. fast shifts of eye, head, and arm positions, where the eye moves faster than head and arm

[2] This equation follows from the group properties of quaternion vectors

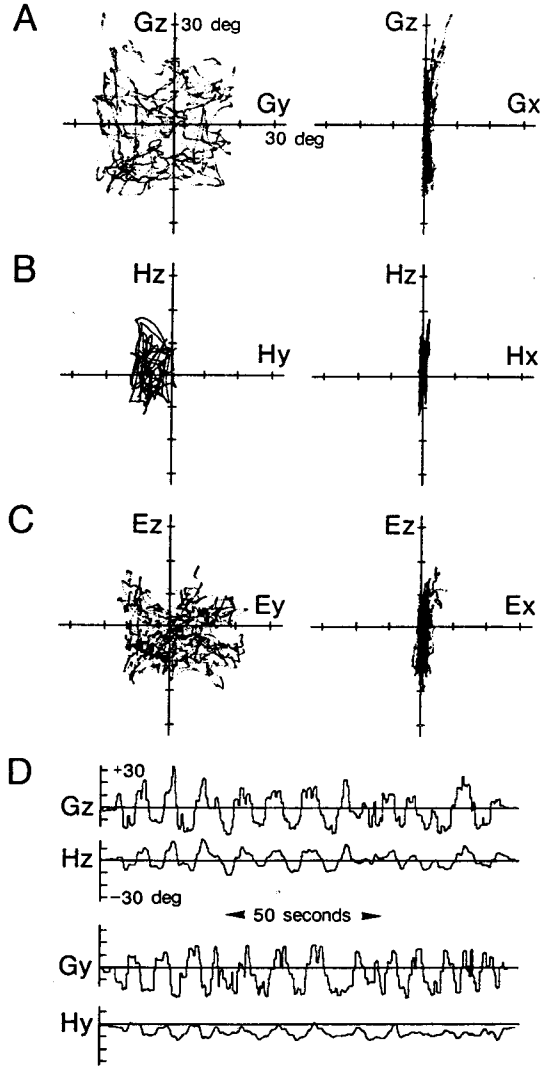

Fig. 2A–D. Example of gaze saccades. Run duration: 50 s. Eye and head rotations relative to the magnetic frame were measured simultaneously. Eye-in-head rotation is calculated from eye-in-space and head-in-space. Rotatory trajectories relative to the magnetic field configuration are described by means of quaternion vectors. The graph shows two views of the three-dimensional coordinate system. The observer is rotated by 90 deg from one view to the other. **A** Eye-in-space (=Gaze) trajectories. 1st column: front view (Gy-Gz-plane); 2nd column: side view (Gx-Gz-plane). Standard deviation from best-fit plane (SD): 1.0 deg. **B** Head-in-space trajectories; front (Hy-Hz-plane) and side (Hx-Hz-plane) view. SD: 0.7 deg. Angle between the planes of gaze and head: 2.3 deg. **C** Eye-in-head trajectories as computed from eye-in-space and head-in-space; front (Ey-Ez-plane) and side (Ex-Ez-plane) view. SD: 1.2 deg. **D** Horizontal and vertical rotatory components of gaze and head. Gz: horizontal gaze component; Hz: horizontal head component; Gy: vertical gaze component; Hy: vertical head component

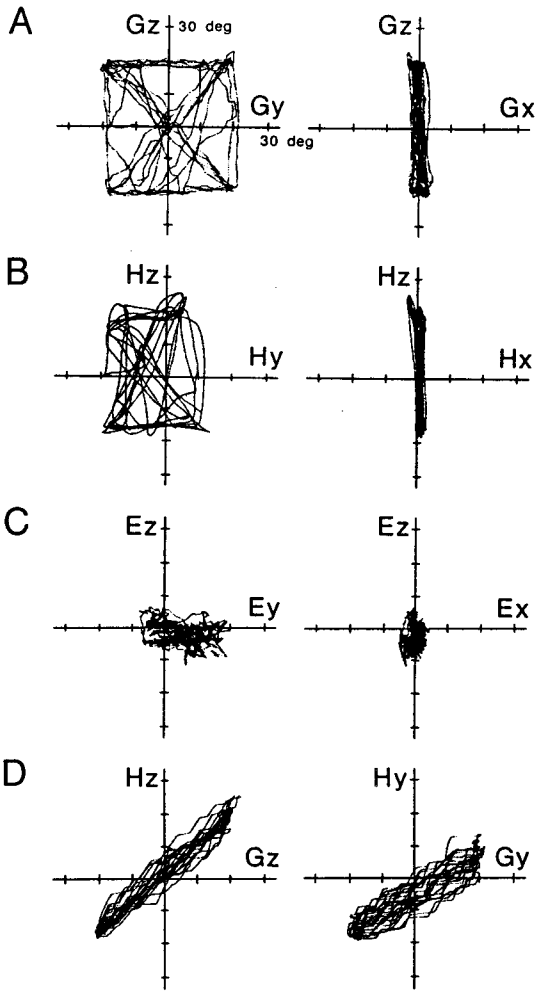

Fig. 3A–D. Example of gaze pursuit. **A** Eye-in-space (=Gaze) trajectories. 1st column: front view (Gy-Gz-plane); 2nd column: side view (Gx-Gz-plane). Standard deviation from best-fit plane (SD): 1.2 deg. **B** Head-in-space trajectories; front (Hy-Hz-plane) and side (Hx-Hz-plane) view. SD: 1.0 deg. Angle between the planes of gaze and head: 2.9 deg. **C** Eye-in-head trajectories as computed from eye-in-space and head-in-space; front (Ey-Ez-plane) and side (Ex-Ez-plane) view. SD: 1.0 deg. **D** Gaze vs. head trajectories. 1st column: correlation between the horizontal gaze (Gz) and the horizontal head (Hz) component. 2nd column: Correlation between the vertical gaze (Gy) and the vertical head (Hy) component

tal (z-axis) and vertical (y-axis) rotations. Although eye movements are much faster than head movements, the gaze and head trajectories, displayed in time-dependence (2D), appear to be strongly correlated in their respective planes.

Figure 3 shows the quaternion vectors of a typical run of gaze pursuit (=pursuit with the head unrestrained). The subject visually follows a moving laser dot on the screen. Gaze (3A) and head (3B) trajectories are confined to Listing planes, while eye-in-head (3C) stays close to the primary position, except for downward rotations. This indicates that most of the gaze movement during pursuit is performed by the head. The horizontal and vertical components of gaze and head are linearly related (3D). For the horizontal correlation the slope is almost unity since the horizontal gaze component is mainly due to head movements. The slope for the vertical correlation is not as steep because the contribution of the eye-in-head rotation to the gaze rotation is larger in this direction.

To determine how well rotatory trajectories are confined to a plane, one can quantify the "thickness" of the data cloud by computing the standard deviation of all sampled data points from a least-square fitted plane. The Listing planes for eye-in-space and head-in-space rota-

tions were almost equally thick: The mean value over all subjects for eye-in-space was 1.4 ± 0.5 deg (range: 0.8–2.3, $n = 15$); the mean value for head-in-space was 1.3 ± 0.5 deg (range: 0.7–1.9, $n = 15$).

For eye-in-head planes, we studied static and dynamic situations: Static: When subjects kept their heads fixed in different horizontal (yaw ± 20 deg) and vertical positions (pitch ± 15 deg) and looked around on the screen, eye-in-head rotations were effectively confined to head-fixed planes, which were as thin as the plane for eye rotations relative to space with the head upright (1.3 ± 0.3 deg, range: 0.6–1.5, $n = 14$). Dynamic: during gaze pursuit, subjects kept their eyes near the primary position, and the head performed most of the movement. Therefore no statistically significant plane could be fitted through these eye-in-head rotation data (example in Fig. 3). During saccadic head-unrestrained gaze shifts, eye-in-head planes were again head-fixed, as in the static case, but slightly thicker (1.6 ± 0.3 deg, range: 1.1–2.2, $n = 10$) than the corresponding eye-in-space planes (example in Fig. 2). The analysis of eye and head trajectories with high spatial and temporal resolution (not shown) revealed that this small increase in thickness is due to compensatory eye movements induced by head rotations: The vestibulo-ocular reflex (VOR) tends to drive the eye out of its head-fixed Listing plane. But, since in all subjects the angle between the planes of eye-in-space and head-in-space never exceeded 6.5 deg (3.6 ± 1.4, range: 1.7–6.5, $n = 14$), compensatory eye movements were mainly induced in the horizontal and vertical, scarcely in the torsional direction. Thus, the disrupting effect of the VOR on the eye-in-head plane is minimized by implementing head and gaze planes almost in parallel.

Having found that the eye-in-head Listing plane was head-fixed both during static head positions and head-unrestrained saccadic gaze shifts, we investigated whether the planes for head-in-space and eye-in-space rotations were body-fixed. To answer this question, we rotated the body between runs about the vertical axis, while the workspace was kept stationary. Tasks were repeated for each body-position. Surprisingly, the gaze and head Listing planes did not change their average orientation relative to the screen, even though body and shoulders were turned up to 30 deg. Fig. 4 shows the horizontal angles between the head Listing planes and the screen. Frontal body position: 1.9 ± 2.4 deg (range: -2.3 to 5.7, $n = 15$); body turned 30 deg to the left: 0.0 ± 3.8 deg (range: -9.1–4.6, $n = 15$); body turned 30 deg to the right: 3.3 ± 6.1 deg (range: -4.0 to 13.5, $n = 13$). If the head Listing plane were body-fixed, it should turn 15 deg when the body orientation is changed by 30 deg (dashed line)[3]. These data indicate that, for gaze and head movements in a selected part of the full workspace, there are Listing planes which are rather space-fixed than body-fixed; we shall call them "workspace-oriented local Listing planes". In one person we noticed that the head Listing plane was almost body-fixed for body rotations to the right side (see the three filled triangles close to the dashed line in Fig. 4) but workspace-oriented for rotations to the left side. By closer examination of the subject's neck motility, we found that the range of head movements to the right was 10 deg smaller than to the left.

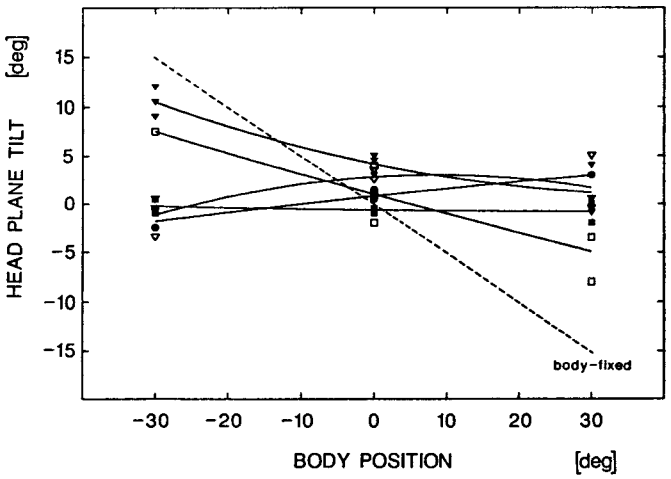

Fig. 4. Horizontal angle between the head Listing plane and the screen as a function of body position. Subjects had to point with a head-fixed laser to dots displayed on the screen. Run duration: 50 s. Abscissa: horizontal angle between the frontal body plane and the screen (in deg). Ordinate: horizontal angle between the head Listing plane and the screen (in deg). The symbols denote data points for the five subjects and are connected using a second order regression to show possible tendencies of plane tilt. The *dashed line* specifies the amount of angular displacement that should result if the head Listing planes were body-fixed. Statistical values are given in the text

In a second set of experiments, we studied arm rotations and, in particular, gaze-arm and head-arm synergies during visually guided arm movements. Figure 5 shows the quaternion vectors of a simultaneous recording of gaze (5A) and right arm (5B) rotations during saccadic pointing to laser dots within ± 25 deg around the center of the screen. The elbow is kept in a naturally extended position with an angle of about 150 deg, and the upper arm is directed essentially forward. One clearly sees Listing planes for gaze and arm; the close correspondence of gaze and arm trajectories in direction and amplitude is shown in the time-dependent traces (5C).

Figure 6 represents the quaternion vectors of a simultaneous recording of gaze (6A) and right arm (6B) rotations during pursuit pointing towards a moving laser dot on the screen. Again, the trajectories for gaze and arm lie in Listing planes. The close correspondence of gaze and arm trajectories in direction and time is demonstrated by the correlation of horizontal and vertical components of gaze and arm (6C). Since both rotatory systems stay on target, the slopes for the horizontal and vertical correlations are close to unity.

Arm Listing planes are about two times thicker than gaze, head, or eye Listing planes (1.8 ± 0.5 deg, range: 0.8–2.7, $n = 19$)[4]. Given the full torsional range of rota-

[3] Due to the properties of quaternion vectors, the angle between planes of quaternion vectors corresponds to a shift of the primary directon by twice the angle (Tweed et al. 1990)

[4] In our complete data base of right and left arm movements ($n = 198$) with various fixed grips, different shoulder-hand distances and body positions the values were 2.0 ± 0.6 deg

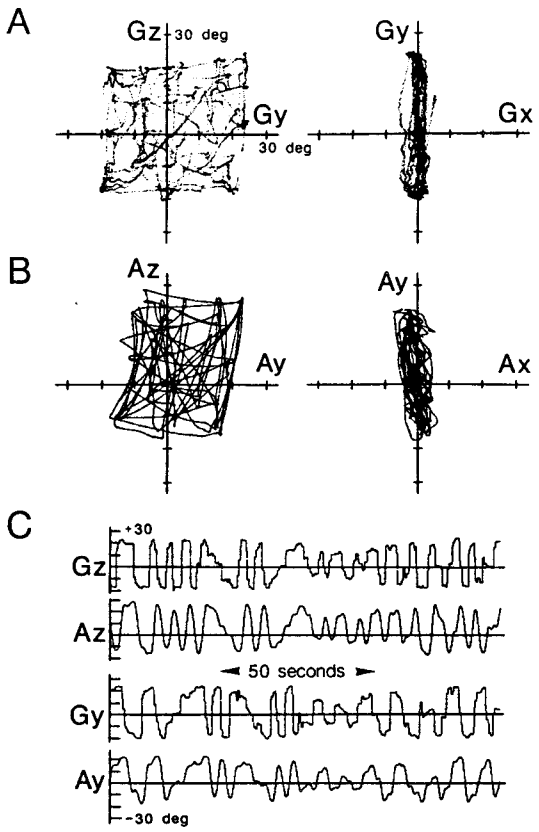

Fig. 5A–C. Example of gaze and arm trajectories during saccadic pointing to dots on the screen. Run duration: 50 s **A** Eye-in-space (=Gaze) trajectories. 1st column: front view (Gy-Gz-plane); 2nd column: top view (Gx-Gy-plane). Standard deviation from best-fit plane (SD): 1.7 deg. **B** Arm-in-space trajectories; front (Ay-Az-plane) and top (Ax-Ay-plane) view. SD: 2.0 deg. Angle between the planes of gaze and arm: 6.1 deg. **C** Horizontal and vertical rotatory components of gaze and arm. Gz: horizontal gaze component; Az: horizontal arm component; Gy: vertical gaze component; Ay: vertical arm component

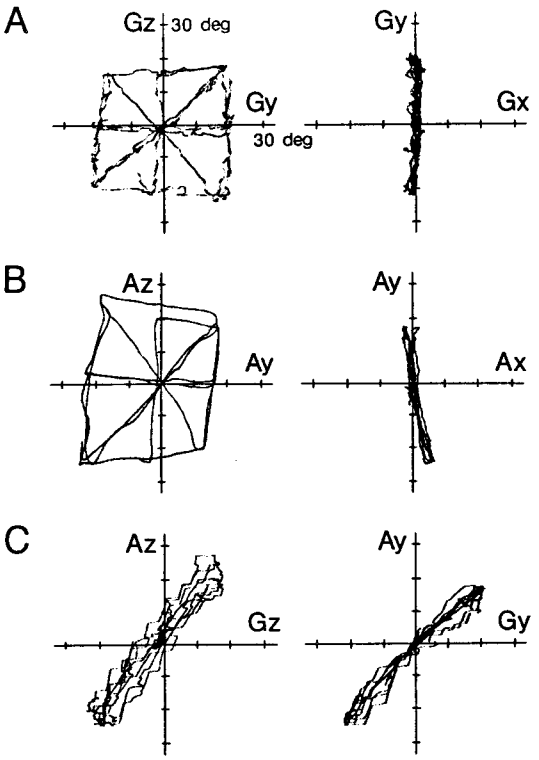

Fig. 6A–C. Gaze and arm movements during pointing to a moving laser dot on the screen (pursuit task). Run duration: 50 sec. **A** Eye-in-space (=Gaze) trajectories. 1st column: front view (Gy-Gz-plane); 2nd column: top view (Gx-Gy-plane). Standard deviation from best-fit plane (SD): 1.0 deg. **B** Arm-in-space trajectories; front (Ay-Az-plane) and top (Ax-Ay-plane) view. SD: 1.3 deg. Angle between the planes of gaze and arm: 11.0 deg. **C** Gaze vs. arm trajectories. 1st column: Correlation between the horizontal gaze (Gz) and the horizontal arm (Az) component. 2nd column: Correlation between the vertical gaze (Gy) and the vertical arm (Ay) component

tion in the shoulder joint, which can exceed 90 deg, this precision is remarkable. In comparison, the maximum torsional range for the eye is only about 30 deg (Balliet and Nakayama 1978) and for the head about 60 deg.

Orientation and thickness of the arm Listing plane did not show major variations with different shoulder-hand distances, i.e. different elbow angles[5]. Constraining the hand orientation by specifying a grip, which oriented the palm downward or sideward, had no significant effect on the orientation of the arm Listing plane. However, for different grips we found idiosyncratic parallel shifts of the plane in the torsional direction. From these shifts, one can determine the contribution of the upper arm to the required hand torsion relative to space. Left and right arm Listing planes were equally thick, and extensive practice did not reduce the thickness of the planes. Furthermore, visual feedback had no effect on the orientation and the shape of the arm plane, i.e. we could not

[5] The elbow angle was varied from trial to trial between a maximally extended position and a position where the shoulder-arm-distance was decreased by 15 cm

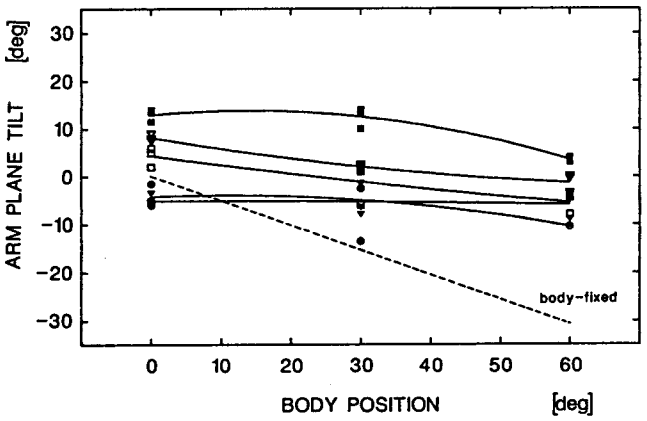

Fig. 7. Horizontal angle between the Listing plane of the right arm and the screen as a function of body position. Subjects had to point to dots on the screen. Run duration: 50 s. Abscissa: horizontal angle between the frontal body plane and the screen (in deg). Ordinate: horizontal angle between the arm Listing plane and the screen (in deg). The symbols denote data points for the five subjects and are connected using a second order regression to show possible tendencies of plane tilt. The *dashed line* specifies the amount of angular displacement that should result if the arm Listing planes were body-fixed. Statistical values are given in the text

observe differences between arm planes produced in the light and in the dark. As for gaze and head, the local Listing planes of the arm were workspace-oriented, not body-fixed. Although subjects were turned with their body and shoulders about the vertical axis up to 60 deg relative to the center of the workspace, the arm plane kept nearly the same orientation. The mean horizontal angle between arm Listing planes and the tangent screen did not exceed 10 deg, regardless of the body position. Figure 7 shows the horizontal angles between the right arm Listing planes and the screen. Frontal body position: 3.7 ± 8.0 deg (range: -6.8–15.6, $n=15$); body turned 30 deg to the left: 0.7 ± 8.4 deg (range: -15.1–15.6, $n=15$); body turned 60 deg to the left: -4.0 ± 5.5 deg (range: -11.9–4.6, $n=14$). If the arm Listing plane were body-fixed, it should turn by 30 deg when the body orientation had changed by 60 deg. With extreme turning of the body relative to the workspace, we observed a tendency of the arm plane to tilt in the same direction. However, without going to the biomechanical limits of the shoulder, the arm Listing plane stayed approximately workspace-oriented[6].

In all subjects, the angles between head and arm planes, and therefore between gaze and arm planes, were small. The head-arm-angle was 7.5 ± 4.0 deg (range: 2.7 to 15.5, $n=18$). This angle, together with the even smaller gaze-head-angle, is a measure of the spatial alignment of the three Listing planes during stereotyped synergies for visually guided movements. During coordinated eye-head-arm rotations, the trajectories in these planes are strongly related: In saccadic movements, head and arm follow gaze; in pursuit movements, all three systems are in a narrow spatio-temporal correspondence.

Discussion

We found that during coordinated eye-head-arm rotations the quaternion vectors of gaze, head and arm lie in planes, called Listing planes. These planes are closely aligned, and the trajectories in the planes correlate linearly in direction and amplitude. However, while in pursuit tasks this correlation holds during the entire time course, head and arm lag the eye in saccadic tasks. The purpose of Listing's law for eye, head, and reaching movements can be understood from Bernstein's concepts on motor synergies: On the level of each subsystem, the brain tries to perform rotatory movements by using the smallest possible number of control parameters. This seems to be done with the following two strategies: (1) The torsional component of each angular position is a function of the horizontal and vertical components, e.g. the amount of arm torsion is determined by the direction of reaching. For the eye, this property was described by Donders (1848). (2) Two such positions can be connected by a fixed-axis rotation along positions which fulfill the first requirement. Geometrically, these two principles lead to rotatory trajectories which lie in a Listing plane (Hepp 1990).

When eye and head are coupled in gaze, or gaze and arm are coupled in reaching and grasping, the progressive reduction of the degrees of freedom to almost parallel Listing planes for gaze, head, and arm effectively results in a two-dimensional control space, which the central nervous system can utilize to simplify eye-head-arm-coordination. If all three systems – eye, head and arm – operate within Hering's "engerem Blickraum" (1868)[7], in which most natural movements occur, the observed pattern of eye-head-arm-coordination generalizes the coordinative eye-head dynamics found by Bizzi et al. (1981) in their basic studies of gaze in the periprimary range.

The Listing planes for gaze, head and arm are local and workspace-oriented, i.e. depending on the center of the workspace, the directional position of gaze, head or arm leads to a different torsional component. This phenomenon actually excludes the existence of a "global Listing plane". According to recent findings of Georgopoulos et al. (1988), Kalaska et al. (1990) and Caminiti et al. (1990), the directional coding of movement and force in neurons of the cortical motor arm region are workspace-, not body-centered, because in the spherical mean over a population of neurons, the on-direction rotates by almost the same amount as the center of the monkey's reaching workspace. As an advantage of workspace-oriented implementations of head and arm motor control, the appropriate reaching synergies can be addressed on the level of the spinal cord by the same cortical population, independent of the position of the limb. In addition, the sensorimotor transformation from the visual input, which per se is invariant of the body position, to the motor output can be simplified by workspace-oriented motor control parameters. For more details concerning the relation of vision, gaze movements and reaching synergies see Hepp et al. (1991).

In robotics, the control of redundant degrees of freedom in multi-joint manipulators is a well known problem (Brady et al. 1982). Local workspace-oriented Listing planes provide a clear rationale for constraining the joint rotations for trajectories of a grasping device in an obstacle-free Euclidean space and relate them in a simple way to vision.

Acknowledgements. We thank our colleagues V. Henn, B.J.M. Hess, and A.J. van Opstal for useful advice, and L.E. Miller and M.M.H.J. Teeuwen for fruitful collaboration. The Neurology Department is supported by grants from the Swiss National Foundation nos. 3100–28008.89 and 3199–25239 (ESPRIT MUCOM 3149), the EMDO-Foundation Zürich, and the Sandoz Foundation, Basel.

References

Balliet R, Nakayama K (1978) Training of voluntary torsion. Invest Ophthalmol Vis Sci 17:303–314

Bernstein N (1967) The co-ordination and regulation of movements. Pergamon Press Oxford

[6] In the complete data base of right arm movements at different body positions with constant shoulder-hand distances and constant grips ($n=166$), the horizontal angle between the arm Listing plane and the frontal body plane was -1.8 deg (range: -10.1–6.6)

[7] Literal translation: "restricted gaze space", i.e. gaze excursions up to about ± 20 deg from the forward direction

Bizzi E (1981) Eye-head coordination. In: Brooks VB (ed) Handbook of physiology: the nervous system. Am Physiol Soc, Bethesda pp 1321–1336

Brady JM, Hollerbach JM, Johnson TL, Lonzano-Peres T, Mason MT (eds) (1982) Robot motion: planning and control. MIT Press, Cambridge

Caminiti R, Johnson PB, Urbano A (1990) Making arm movements within different parts of space: dynamic aspects in the primate motor cortex. J Neurosci 10:2039–2058

Donders FC (1848) Beitrag zur Lehre von den Bewegungen des menschlichen Auges. Holländ Beitr Anat Physiol Wiss 1:104–145

Ferman L, Collewijn H, Van den Berg AV (1987) A direct test of Listing's law: II. Human ocular torsion measured under dynamic conditions. Vision Res 27:939–951

Georgopoulos AP, Kettner RE, Schwartz AB (1988) Primate motor cortex and free arm movements to visual targets in three-dimensional space. II. Coding of the direction of movement by a neuronal population. J Neurosci 8:2928–2937

Helmholtz H von (1866) Handbuch der physiologischen Optik. Voss, Hamburg. Engl transl: (1962) Helmholtz' Treatise on physiological optics. Dover, New York

Hepp K (1990) On Listing's law. Comun Math Phys 132:285–292

Hepp K, Haslwanter T, Straumann D, Hepp-Reymond M-C, Henn V (1991) The control of arm, gaze and head by Listing's law. In: R Caminiti (ed) Control of arm movement in space: neurophysiological and computational approaches. Exp Brain Res Suppl (in press)

Hepp K, Hepp-Reymond MC (1989) Donders' and Listing's law for reaching and grasping arm synergies. Soc Neurosci Abstr 15:604

Hering E (1868) Die Lehre vom binocularen Sehen. Engelmann, Leipzig

Jeannerod M (1988) The Neural and behavioural organization of goal-directed movements. Clarendon, Oxford

Kalaska JF, Cohen DA, Prud'homme M, Hyde ML (1990) Parietal area 5 neuronal activity encodes movement kinematics, not movement dynamics. Exp Brain Res 80:351–364

Robinson DA (1963) A method of measuring eye movements using a search coil in a magnetic field. IEEE Trans Biomed Eng 10:137–145

Tweed D, Vilis T (1987) Implications of rotational kinematics for the oculomotor system in three dimensions. J Neurophysiol 58:832–849

Tweed D, Vilis T (1988) Listing's law for the head. Soc Neurosci Abstr 14:958

Tweed D, Vilis T (1990) Geometric relations of eye position and velocity vectors during saccades. Vision Res 30:111–127

Westheimer G (1957) Kinematics of the eye. J Optic Soc Am 47:967–974